

Partially coherent phonon heat conduction in superlattices

B. Yang* and G. Chen†

Mechanical Engineering Department, Massachusetts Institute of Technology, Massachusetts 02139
(Received 21 October 2002; revised manuscript received 23 December 2002; published 8 May 2003)

In this paper, the phonon thermal conductivity of semiconductor superlattices is calculated with the use of a modified lattice dynamics model, in which an imaginary wave vector is added. The mean free path caused by diffuse interface scattering is included in the imaginary wave vector. This model combines the effects of phonon confinement and diffuse interface scattering on the thermal conductivity in superlattices, and is applicable to phonon transport in the partially coherent regime, where bulk and superlattice phonon modes mix up. The theoretical results for the GaAs/AlAs superlattices are compared with the experimental data. The period thickness dependence and temperature dependence of the thermal conductivity in the GaAs/AlAs superlattices can be well explained by this model.

DOI: 10.1103/PhysRevB.67.195311

PACS number(s): 68.65.-k, 66.70.+f, 44.05.+e

Phonon thermal conductivity in semiconductor superlattices (SL's) has attracted considerable attention due to the applications in thermoelectric devices¹⁻⁵ and optoelectronic devices such as quantum well lasers and detectors.^{6,7} The thermal conductivities both parallel (in-plane) and perpendicular (cross-plane) to the interfaces are found to be significantly reduced in comparison to their corresponding bulk values in various SL groups.⁸⁻¹⁴ Some experimental data show that the cross-plane thermal conductivity recovers in the short period limit, hence a minimum thermal conductivity occurs.^{11,12} Many theoretical models for phonon transport in SL's have been developed, but the mechanisms of the thermal conductivity reduction are still under debate.

Current models on phonon transport in SL's generally fall into two groups. One group assumes that the phonon mean free path (MFP) is shorter than the period thickness so that phonons in different layers of a SL are not coherently correlated and each layer is subject to its bulk dispersion relations.^{3,15-17} In this case, phonons are in the totally incoherent regime, and can be treated as particles. The thermal conductivity is usually calculated using the Boltzmann transport equation with boundary conditions involving diffuse interface scattering. These particle models can fit experimental data of several SL systems in the thick period range. Because the wave features of phonons in SL's are not considered, they fail to explain the thermal conductivity recovery in the short period limit.

The other group assumes that the phonon MFP is much larger than the SL period thickness.^{2,18-21} So phonons in different layers of a SL are coherently correlated and SL phonon bands can be formed due to the coherent interference of the phonon waves transporting towards and away from the interfaces. Phonon transport in such wave models is in the totally coherent regime. The thermal conductivity in SL's is usually calculated through the phonon dispersion relation in SL's, obtained using lattice dynamics or other methods, and the relaxation time in the corresponding bulk materials. The thermal conductivity of SL's calculated from these models typically first decreases with increasing period thickness and then approaches a constant with the period thickness beyond about 10 monoatomic layers (ML's). The very thin period behavior is similar to some experimental observations, but

the thick period behavior is contrary to the experimental results observed in many SL groups, such as GaAs/AlAs and Bi₂Te₃/Sb₂Te₃, which show an increase in thermal conductivity with increasing period thickness.^{8,11,12,22}

Apparently, neither coherent wave models nor incoherent particle models alone can explain the period thickness dependence of thermal conductivity in SL's because each of them deals with the extreme case. In reality, phonon transport in SL's can fall into either coherent regime or incoherent regime or in between, depending on phonon MFP and period thickness. General approaches applicable to phonon transport in the partially coherent regime in SL's are needed.

Simkin and Mahan employed a simple-cubic lattice dynamics model with a complex wave vector involving MFP, to calculate the SL thermal conductivity.²³ This idea was originally proposed by Pendry for the electron energy band.²⁴ The addition of an imaginary part to the wave vector is a phenomenological way to include the effects of the finite MFP on phonon modes in SL's. In Ref. 23, they calculated the period thickness dependence of thermal conductivity in the cross-plane direction of SL's, and predicted a minimum in the cross-plane thermal conductivity. However, their model did not consider the diffuse interface scattering. As a consequence, the model cannot explain the in-plane thermal conductivity reduction in SL's. Even in the cross-plane direction, the calculated maximum thermal conductivity reduction is similar to that predicted by the coherent lattice dynamics models and is still many times smaller than the experimental data.

In this paper, a treatment combining Simkin and Mahan's model²³ and diffuse interface scattering^{3,16,17,25,26} is developed to investigate the thermal conductivity in SL's. With this treatment, the experimentally observed thermal conductivity reduction along both in-plane and cross-plane directions of SL's can be explained over all the period thickness range. The temperature dependence of thermal conductivity in SL's can also be explained.

The thermal conductivity in the GaAs/AlAs SL's is calculated with the use of a modified face-centered-cubic lattice dynamics model.^{18,21} More accurate lattice dynamics models, considering long-range force and optical phonons, show similar results.^{19,20} The traditional lattice dynamics models

are applicable only when the MFP is much larger the period thickness of SL's. To study partially coherent phonons in SL's, an imaginary part, i/MFP_{SL} , is added to the wave vector in the lattice dynamics model. The MFP caused by diffuse interface scattering is derived and incorporated into the total phonon MFP, MFP_{SL} . Here it is assumed that scattering processes destroy the phonon phase and thus the phonon MFP is identical to phonon coherent length. Compared to the lattice dynamics models in Refs. 18 and 21, a modification is that not only the mass difference but also the force constant difference between GaAs and AlAs are considered. The parameters are taken from Refs. 18 and 21 except that the force constants in GaAs layers and AlAs layers are chosen as 33.5 K g/s^2 and 33.3 K g/s^2 , respectively.

In SL's, phonon scattering may happen at interfaces due to diffuse interface scattering, and within the layers due to internal volumetric scatterings such as Umklapp scattering. According to Mathiessen's rule, the total MFP in SL's is $\text{MFP}_{\text{SL}} = 1/(1/\text{MFP}_i + 1/\text{MFP}_d)$, where MFP_i and MFP_d are the MFP's of internal volumetric scattering and diffuse interface scattering, respectively.²⁷ Interface roughness is generally considered as the source of diffuse interface scattering. It is known that even the best-grown semiconductor SL's, such as GaAs/AlAs, have large flat terraces with edge of 1–2 ML's at interfaces.²⁸ We employ a simple description to the interface scattering, according to which a fraction P of the incident phonons are specularly scattered while the remainder $(1-P)$ are diffusely scattered in all directions isotropically.²⁹ Although many studies have been conducted in literature on thermal boundary resistance, there is no simple way to calculate the specularity parameter P .²⁶ In this work, P is treated as a fitting parameter. We consider the situation that a phonon passes through the interfaces of a SL at an incident angle of θ to the normal. The spacing of interfaces is d and the specularity parameter of each interface is P . The possibility that the phonon will not be diffusely scattered after traveling a distance x is $P^x \cos(\theta)/d$. Thus, the MFP caused by the interface diffuse scattering takes the form²⁷

$$\text{MFP}_d = -d/\cos(\theta)\ln(P), \quad (1)$$

where $P > 1/e$ because the MFP_d cannot be smaller than the layer thickness d .

It has been reported that the change in Umklapp scattering rate in SL's is modest (at most 25%).³⁰ So if the change in the internal scattering rate in the SL's is ignored, the total MFP in SL's takes the value

$$\text{MFP}_{\text{SL}} = 1/(1/\text{MFP}_{i,B} + 1/\text{MFP}_d), \quad (2)$$

where $\text{MFP}_{i,B}$ is the phonon MFP of the corresponding bulk materials. Another assumption made in the calculation is that MFP_d for the $1 \text{ ML} \times 1 \text{ ML}$ and $2 \text{ ML} \times 2 \text{ ML}$ SL's approximates to the value for the $3 \text{ ML} \times 3 \text{ ML}$ SL. This is because the interfaces tend to be indistinct in the $1 \text{ ML} \times 1 \text{ ML}$ and $2 \text{ ML} \times 2 \text{ ML}$ GaAs/AlAs SL's due to the 1–2 ML's transition region at interfaces.

The comparison between the MFP's caused by diffuse interface scattering and by bulk internal scattering is shown in Figs. 1(a) and 1(b). The $\text{MFP}_{i,B}$ is the average MFP for

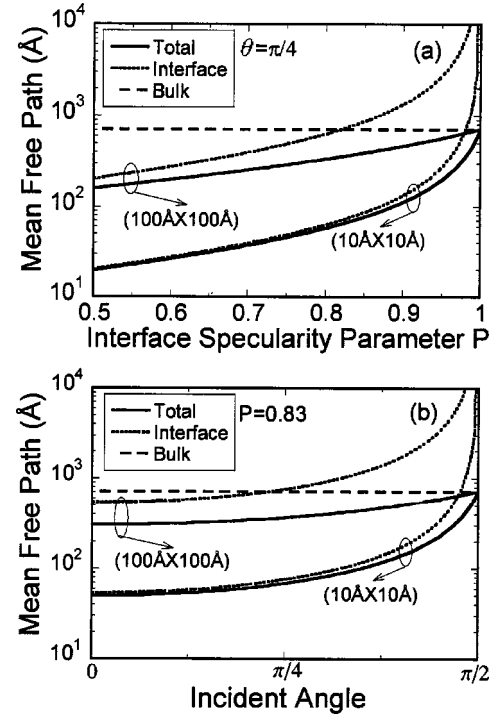


FIG. 1. Phonon MFP in GaAs/AlAs SL's as a function of (a) interface specularity parameter P and (b) incident angle θ . The total MFP includes two parts: MFP same as the corresponding bulk value (labeled "bulk") and MFP caused by diffuse interface scattering (labeled "interface").

bulk GaAs and AlAs, and has the value of 716 \AA at room temperature, obtained by fitting the experimental data with the use of the phonon properties calculated from the lattice dynamics model. As seen in these figures, MFP_d is anisotropic and drops with the decreasing incident angle or the decreasing interface specularity parameter P . The total phonon MFP is significantly suppressed due to the diffuse interface scattering. However, this suppression of MFP becomes weaker in the $(100 \text{ \AA} \times 100 \text{ \AA})$ GaAs/AlAs SL than that in the $(10 \text{ \AA} \times 10 \text{ \AA})$ GaAs/AlAs SL.

Figure 2 shows the dispersion curves for phonons propagating in the cross-plane direction in the $2 \text{ ML} \times 2 \text{ ML}$ GaAs/AlAs SL, calculated from lattice dynamics models (a) without and (b) with the addition of the imaginary wave vector. In both cases, the frequency gaps occur at the center and boundary of the folded Brillouin zone and the dispersion curves are flattened, especially at high frequencies. The phonon group velocity in SL's is reduced, but the magnitude of the reduction depends on the band gap width. Comparing Figs. 2(a) and 2(b), it is seen that the introduction of the imaginary wave vector results in the diminishing band gaps. This is consistent with the result of Simkin and Mahan based on a simple-cubic lattice dynamics model.²³ When the imaginary wave vector is large, phonon waves are highly damped and sample only a limited number of unit cells, and thus tend to be subject to the bulk dispersion as the band gaps diminish to zero. When the imaginary wave vector is zero, the lattice waves extend over the whole SL and the new SL bands will form. In the in-plane direction of SL's, the change in the

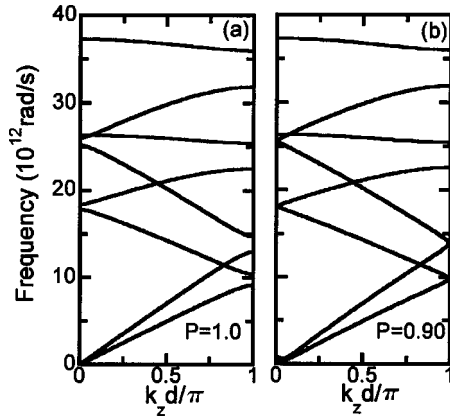


FIG. 2. Dispersion relations of phonons in the cross-plane direction of the 2 ML \times 2 ML GaAs/AlAs SL, calculated from the lattice dynamics model (a) without diffuse interface scattering (perfect interfaces, $P=1$) and (b) with diffuse interface scattering (rough interfaces, $P=0.9$).

band gaps is much smaller due to the much larger in-plane MFP, which is not plotted here.

Based on the dispersion relation, the thermal conductivity is given by^{18,21}

$$K_i = \sum_{\lambda} C_{\text{ph}}(\omega_{\lambda}) \cdot \left| \frac{\partial \omega}{\partial k_i} \right| \cdot \text{MFP}_{\text{SL}}(\theta, T), \quad (3)$$

where λ denotes the SL modes, k is a wave vector, $C_{\text{ph}}(\omega_{\lambda})$ represents the mode specific heat, i identifies the direction of thermal conduction, and T is temperature.

Figure 3 shows the calculated temperature dependence of the thermal conductivity in both in-plane and cross-plane directions of the 2 ML \times 2 ML GaAs/AlAs SL's, along with the reported experimental data and the corresponding bulk values. It is known that the bulk GaAs and AlAs thermal conductivities go as $T^{-\alpha}$ (where α is 1.25 for GaAs and 1.37 for AlAs) in the moderate temperature range due to the pre-

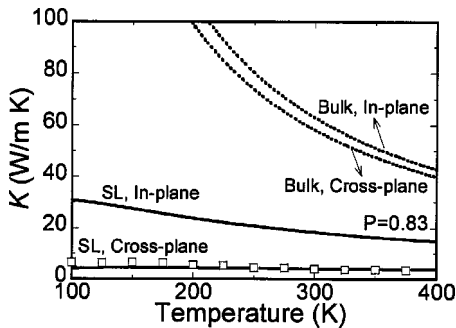


FIG. 3. Temperature dependence of the thermal conductivity in both in-plane and cross-plane directions of the 2 ML \times 2 ML GaAs/AlAs SL, calculated from the modified lattice dynamics model with diffuse interface scattering ($P=0.83$). The dot lines are the effective thermal conductivities based on the Fourier law and the bulk GaAs and bulk AlAs thermal conductivity in literature, i.e., $K_{\text{bulk, in plane}} = (K_{\text{GaAs}} + K_{\text{AlAs}})/2$ and $K_{\text{bulk, cross plane}} = 2K_{\text{GaAs}} \cdot K_{\text{AlAs}} / (K_{\text{GaAs}} + K_{\text{AlAs}})$. The squares (\square) are experimental data by Capinski *et al.* (Ref. 12).

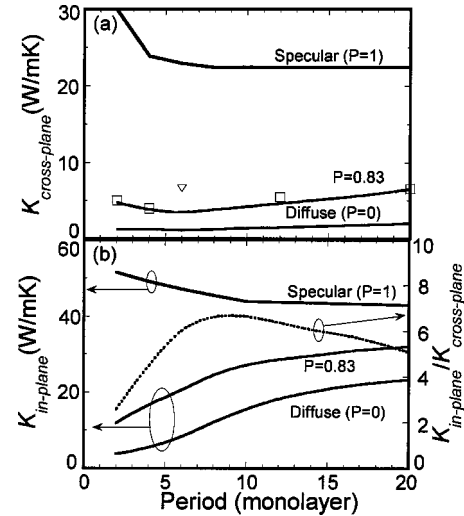


FIG. 4. Calculated thermal conductivity in (a) the cross-plane and (b) in-plane directions of the GaAs/AlAs SL's as a function of the period thickness at room temperature. The thermal conductivity anisotropy ($K_{\text{in-plane}}/K_{\text{cross-plane}}$) for the GaAs/AlAs SL with $P=0.83$ is also plotted in (b). The triangles and the squares represent samples grown at different institutions. All of them were measured by Capinski *et al.* (Ref. 12).

dominating phonon-phonon scattering.^{31,32} The cross-plane thermal conductivities of the 2 ML \times 2 ML GaAs/AlAs SL, however, shows much weaker temperature dependence, which is proportional to $T^{-0.55}$, according to the experimental data by Capinski *et al.*¹² This implies that the effect of the temperature-dependent phonon-phonon scattering is much weaker in the SL relative to that in the corresponding bulk, and the interface scattering that is insensitive to temperature plays a dominant role. The slightly steeper slope of the in-plane thermal conductivity indicates that the effects of the diffuse interface scattering on the phonon transport in the cross-plane direction is stronger than that in the in-plane direction.

Figure 4 shows the calculated thermal conductivity as a function of the period thickness at room temperature ($T=300$ K) in both in-plane and cross-plane directions of the GaAs/AlAs SL's, along with the reported experimental data for comparison. The results calculated with perfect interfaces ($P=1$) are the same as those from the traditional lattice dynamics models, and are not in agreement with the experimental data.¹² However, the experimental data can be well explained by the introduction of diffuse interface scattering ($P=0.83$) to lattice dynamics model. These results are consistent with the results based on molecular dynamics simulation, which also shows the rough interfaces significantly decrease the thermal conductivity in SL's.³³ The recovery of thermal conductivity in the extremely short period is a result of phonon tunneling.^{21,34} The anisotropy of the thermal conductivity ($K_{\text{in-plane}}/K_{\text{cross-plane}}$) is found to be around 5, as seen in Fig. 4(b). There is no experimental report about the anisotropy of thermal conductivity in GaAs/AlAs SL's, however, a few experiments show that the thermal conductivity anisotropies in GaAs/GaAlAs(Ref. 35) and Si/Ge SL's (Refs. 13 and 36) have similar values. A minimum thermal conduc-

tivity occurs in the cross-plane direction for the GaAs/AlAs SL with a period thickness of around 6 ML's, which is a natural result that arises from the combination of lattice dynamics and diffuse interface scattering. The thermal conductivity of Bi₂Te₃/Sb₂Te₃ SL's has also shown this behavior.¹¹

In summary, the thermal conductivity of the GaAs/AlAs SL's has been calculated by a modified lattice dynamics model, in which an imaginary wave vector involving diffuse interface scattering is introduced. This phenomenological approach can apply to phonon transport in the partially coherent regime, as well as the totally coherent and totally incoherent regimes. When the diffuse interface scattering is added to the lattice dynamics model, the experimental data, including period thickness dependence and temperature dependence in both in-plane and cross-plane directions of SL's,

can be well explained. The calculations suggest that both diffuse interface scattering and the modified phonon dispersion are the main causes of the decreased thermal conductivity in the SL's with small period thickness. When the period is large, diffuse interface scattering destroys the phonon coherence such that phonons do not form SL bands. In this case, the thermal boundary resistance at individual interfaces dominates phonon transport until in the very thick limit, where bulk internal scattering turns out to be the dominant factor and thermal conductivity tends to reach the corresponding bulk values.

The authors acknowledge the support from DOD/MURI on thermoelectrics (Grant No. N00014-97-1-0516) and DARPA HERETIC subcontract through JPL.

*Visiting from Mechanical and Aerospace Engineering Department, University of California at Los Angeles.

†Author to whom correspondence should be addressed; electrical address: gchen2@mit.edu

¹L. D. Hicks and M. S. Dresselhaus, Phys. Rev. B **47**, 12 727 (1993).

²P. Hyldgaard and G. D. Mahan, Phys. Rev. B **56**, 10 754 (1997).

³G. Chen, Phys. Rev. B **57**, 14 958 (1998).

⁴R. Venkatasubramanian, E. Siivola, T. Colpitts, and B. O'Quinn, Nature (London) **413**, 597 (2001).

⁵T. C. Harman, P. J. Taylor, M. P. Walsh, and B. E. LaForge, Science **297**, 2229 (2002).

⁶G. Chen, in *Ann. Rev. Heat Transfer* (Hemisphere Pub. Corp., New York, 1996), Vol. 7.

⁷P. Bhattacharya, *Semiconductor Optoelectronic Devices* (Prentice Hall, Upper Saddle River, 1997).

⁸T. Yao, Appl. Phys. Lett. **51**, 1798 (1987).

⁹X. Y. Yu, G. Chen, A. Verma, and J. S. Smith, Appl. Phys. Lett. **67**, 3554 (1995).

¹⁰S. Lee, D. G. Cahill, and R. Venkatasubramanian, Appl. Phys. Lett. **70**, 2957 (1997).

¹¹R. Venkatasubramanian, Phys. Rev. B **61**, 3091 (2000).

¹²W. S. Capinski, H. J. Maris, T. Ruf, M. Cardona, K. Ploog, and D. S. Katzer, Phys. Rev. B **59**, 8105 (1999).

¹³W. L. Liu, T. Borca-Tasciuc, G. Chen, J. L. Liu, and K. L. Wang, J. Nanosci. Nanotech. **1**, 37 (2001).

¹⁴S. T. Huxtable, A. R. Abramson, C. L. Tien, A. Majumdar, C. LaBounty, X. Fan, G. Zeng, J. Bower, and E. T. Croke, Appl. Phys. Lett. **80**, 1737 (2002).

¹⁵G. Chen, ASME J. Heat Transfer **119**, 220 (1997).

¹⁶P. Hyldgaard and G. D. Mahan, in *Thermal Conductivity* (Technomic, Lancaster, PA, 1996), Vol. 23.

¹⁷S. G. Walkauskas, D. A. Broido, K. Kempa, and T. L. Reinicke, J. Appl. Phys. **85**, 2579 (1999).

¹⁸S. Tamura, Y. Tanaka, and H. J. Maris, Phys. Rev. B **60**, 2627 (1999).

¹⁹W. E. Bies, R. J. Radtke, and H. Ehrenreich, J. Appl. Phys. **88**, 1498 (2000).

²⁰A. A. Kiselev, K. W. Kim, and M. A. Stroscio, Phys. Rev. B **62**, 6896 (2000).

²¹B. Yang and G. Chen, Microscale Thermophys. Eng. **5**, 107 (2001).

²²I. Yamasaki, R. Yamanaka, M. Mikami, H. Sonobe, Y. Mori, and T. Sasaki, Proc. ICT' **98**, 210 (1998).

²³M. V. Simkin and G. D. Mahan, Phys. Rev. Lett. **84**, 927 (2000).

²⁴J. B. Pendry, *Low Energy Electron Diffraction* (Academic, New York, 1974).

²⁵H. B. G. Casimir, Physica (Amsterdam) **6**, 495 (1938).

²⁶E. T. Swartz and R. O. Pohl, Rev. Mod. Phys. **61**, 605 (1989).

²⁷B. Yang and G. Chen, Proc. ICT' **02**, 306 (2002).

²⁸T. Ruf, J. Spitzer, V. F. Sapega, V. I. Belitsky, M. Cardona, and K. Ploog, Phys. Rev. B **50**, 1792 (1994).

²⁹J. M. Ziman, *Electrons and Phonons* (Clarendon, Oxford, 2001).

³⁰S. Y. Ren and J. D. Dow, Phys. Rev. B **25**, 3750 (1982).

³¹A. Katz, *Indium Phosphide and Related Materials* (Artech House, Boston, 1992).

³²S. Tiwari, *Compound Semiconductor Device Physics* (Academic, New York, 1992).

³³B. C. Daly, H. J. Maris, K. Imamura, and S. Tamura, Phys. Rev. B **66**, 024301 (2002).

³⁴G. Chen, J. Heat Transfer **121**, 945 (1999).

³⁵G. Chen, C. L. Tien, X. Wu, and J. S. Smith, J. Heat Transfer **116**, 325 (1994).

³⁶B. Yang, W. L. Liu, J. L. Liu, K. L. Wang, and G. Chen, Appl. Phys. Lett. **81**, 3588 (2002).